High-Pressure Investigation of Li_2MnSiO_4 and Li_2CoSiO_4 Electrode Materials for Lithium-Ion Batteries

D. Santamaría-Pérez,*[†,‡] U. Amador,[§] J. Tortajada,[†,‡] R. Dominko,[⊥] and M. E. Arroyo- de Dompablo[¶,‡]

[†]Departamento de Química Física and [¶]Departamento de Química Inorgánica, Facultad de Ciencias Químicas, Universidad Complutense de Madrid, Madrid, Spain

[§]Departamento de Química, Facultad de Farmacia, Universidad CEU—San Pablo, USP-CEU, 28668-Boadilla del Monte, Madrid, Spain

[⊥]National Institute of Chemistry, Hajdrihova 19, SI-1000 Ljubljana, Slovenia
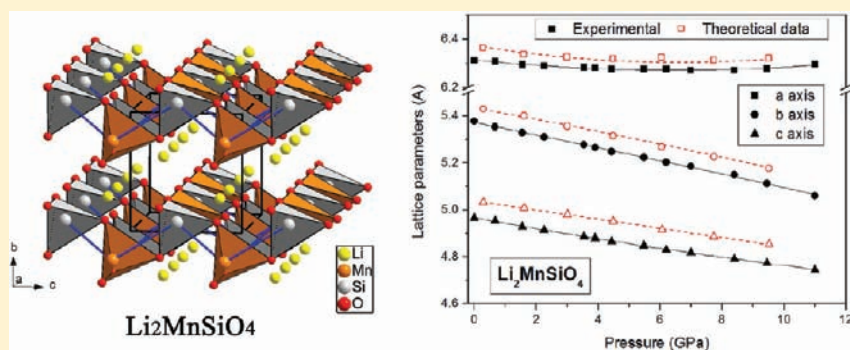
ABSTRACT: In this work, the high-pressure behavior of $Pmn2_1$-Li_2MnSiO_4 and $Pbn2_1$-Li_2CoSiO_4 is followed by in situ X-ray diffraction at room temperature. Bulk moduli are 81 and 95 GPa for $Pmn2_1$-Li_2MnSiO_4 and $Pbn2_1$-Li_2CoSiO_4, respectively. Regardless of the moderate values of the bulk moduli, there is no evidence of any phase transformation up to a pressure of 15 GPa. $Pmn2_1$-Li_2MnSiO_4 shows an unusual expansion of the a lattice parameter upon compression. A density functional theory investigation yields lattice parameter variations and bulk moduli in good agreement with experiments. The calculated data indicate that expansion of the a lattice parameter is inherent to the crystal structure and independent of the nature of the transition-metal atom (M). The absence of pressure-driven phase transformation is likely associated with the incapability of the Li_2MSiO_4 composition to adopt denser structures while avoiding large electrostatic repulsions.

1. INTRODUCTION

The development of new cathode materials for lithium-ion batteries is an active field trying to satisfy the increasing energy demand. Higher energy density could be achieved by increasing either the lithium intercalation voltage or the amount of lithium ions/electrons (capacity) storage in the cathode electrode material. The capacity delivered by commercialized batteries comes from a redox reaction involving the exchange of only one electron (or lithium ion) per formula unit. The silicates Li_2MSiO_4 (where M is a transition metal) emerged in 2005 as promising high-energy cathode materials because of the theoretical possibility of exchanging two electrons per M. In spite of the initial expectations, to date the reversible deintercalation of the two lithium ions per formula unit has not been achieved for any transition-metal ion or their alloys (see ref 1 and references cited therein). Several handicaps for an optimal electrode performance have been identified: too high oxidation voltage for the second lithium ion for most M, low electronic and ionic conductivity, and structural instability of the delithated phases.[2−5] For some M, the latter is directly related to the crystal-field stabilization energy in the tetrahedral environment of the crystal structure.

The crystal structure of Li_2MSiO_4 consists of a distorted hexagonal packing of oxygen ions with half of the tetrahedral sites occupied by lithium, M, and silicon.[6] Informative illustrated surveys of the structures of these and other crystalline silicates are published.[1,7,8] A large number of Li_2MSiO_4 polymorphs would be possible by assuming a different pattern of occupancy of the tetrahedral voids in the distorted hexagonally packed anion framework, similar to the enumeration of dipolar tetrahedral structures in wurtzite-BeO.[9] Given the small energy difference among polymorphs, the obtention of a particular polymorph depends on subtle details of the synthesis conditions.[10−14] Figure 1 shows the structures of the Li_2MSiO_4 polymorphs crystallizing in the $Pbn2_1$ (top) and $Pmn2_1$ (bottom) space groups. The $Pbn2_1$ polymorph is regarded as the most stable form of Li_2MSiO_4 (M = Co, Zn, Mg) but has never been found for Li_2MnSiO_4. The structure consists of parallel chains of alternating $[LiO_4]$ and $[M(Si)O_4]$ tetrahedra along the a axis (see Figure 1a). A better description of the structure arises from application of the extended Zintl—
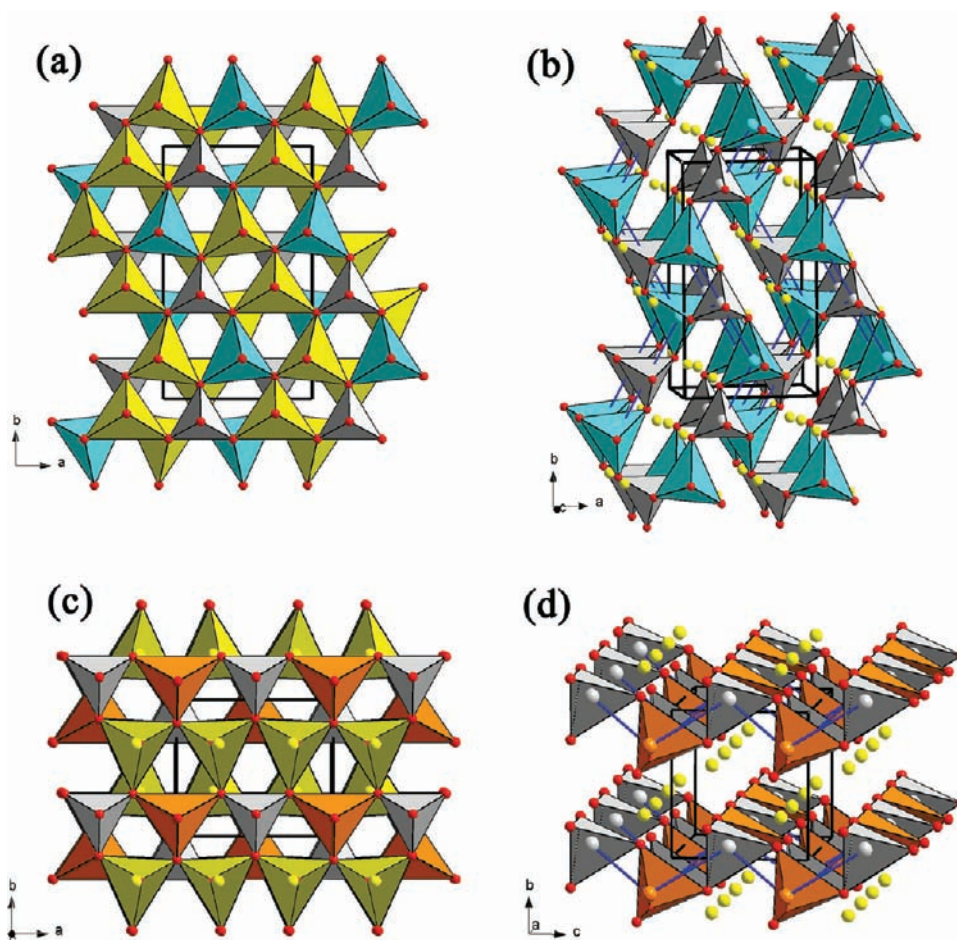
Figure 1. (a) Crystal structure of the Li_2CoSiO_4 polymorph crystallizing with space group $Pbn2_1$. (b) 3D framework of the $[CoSiO_4]^{2-}$ anion consisting of four- and eight-membered rings similar to those of compounds $Rb[AlSiO_4]$ and $Li(H_2O)[AlSiO_4]$. (c) Crystal structure of the Li_2FeSiO_4 polymorph crystallizing with space group $Pmn2_1$. (d) Layers formed by the $[FeSiO_4]^{2-}$ anion. Color code: Li, yellow; Co, cyan; Fe, orange; Si, gray; O, red.

Klemm concept.[15,16] If the lithium atoms would provide two electrons to the 3D framework formed by $[CoO_4]$ and $[SiO_4]$ tetrahedra, the $[CoSiO_4]^{2-}$ anion would be equivalent to a group 14 oxide. Thus, although no phase of a group 14 oxide is known to have this structure of four- and eight-membered rings (see Figure 1b), it is similar to that adopted by the $[AlSiO_4]^-$ polyanion in the ABW-type zeolites $Rb[AlSiO_4]$[17] or $Li(H_2O)$-$[AlSiO_4]$.[18] The structure also resembles that of feldspar, another major group of tectosilicates. Thus, although Li_2MSiO_4 is usually described as an orthosilicate, it should rather be considered as a tectosilicate with half of the silicon/aluminum ions replaced by M ions. Parts c and d of Figure 1 show the crystal structure of the denser polymorph $Pmn2_1$, which is commonly found in the synthesis of Li_2MnSiO_4 and Li_2FeSiO_4. It can be described as built up from infinite corrugated layers of composition $[SiMO_4]_\infty$ lying on the ac plane and linked along the b axis by $[LiO_4]$ tetrahedra. Within these layers, each $[SiO_4]$ tetrahedron shares its four corners with four neighboring $[MO_4]$ tetrahedra, and vice versa (see Figure 1d). To the best of our knowledge, no mineral with this structure is known. Nevertheless, it is important to remark about the similarity between the Mn(Fe)-Si subarray of our silicate and the structure of lead monoxide, PbO, a II−VI compound (mineral litharge).[19] As shown in Figure 1a,c, a clear distinction between

$Pbn2_1$ (top) and $Pmn2_1$ (bottom) can be made by looking along the [001] direction.[10,20]

The structures of all Li_2MSiO_4 polymorphs known to date are built up from $[SiO_4]$, $[LiO_4]$, and $[MO_4]$ tetrahedral units. This tetrahedral coordination was soon identified as a drawback for optimal electrochemical performance;[2,4,13,21] there is a strong driving force for most M^{3+} and M^{4+} ions to change coordination upon lithium extraction and the structure of $Li_{2-x}MSiO_4$ to transform into a more stable structure or to collapse. Aiming to prepare novel Li_2MSiO_4 polymorphs consisting of $[MO_6]$ units, we have previously investigated the behavior of Li_2MSiO_4 (M = Mn, Co) under high pressure and high temperature (up to 8 GPa). In those experiments, the sample was first pressurized with pressure and temperature (1173 K) applied for 1 h, following by quenching to ambient conditions. For both Li_2MnSiO_4 and Li_2CoSiO_4, the densest polymorph (space group $Pmn2_1$) was stabilized after quenching from pressures around 4 GPa. No novel polymorphs were detected in the quenched samples. In this work, we have performed in situ X-ray diffraction (XRD) studies at high pressures (up to 15 GPa) and room temperature, which can provide more insight into the high-pressure behavior of the $LiMSiO_4$ family.

2. METHODOLOGY

2.1. Experimental Section. Samples of Li_2MnSiO_4 were prepared using hydrothermal synthesis as previously reported.[22] Samples of Li_2CoSiO_4 were prepared by a combustion route using as reagents lithium and cobalt nitrates and nanosized cristobalite and urea as the fuel for the reaction. Afterward the as-prepared powder was treated at 950 °C for 48 h and quenched to room temperature. XRD characterization of the Li_2MSiO_4 samples was performed using a Bruker D8 high-resolution powder X-ray diffractometer with monochromatic Cu $K\alpha_1$ (λ = 1.5406 Å) radiation obtained with a germanium primary monochromator and equipped with a MBraun PSD-50M position-sensitive detector. The data were collected in the 2θ range between 10 and 70° in steps of 0.015°. Treatment of the XRD patterns was carried out using the *FullProf* program.[23] Because the structures of the title compounds are well established and XRD is not the best technique to deal with structural features related to light atoms such as oxygen, the atomic coordinates and thermal displacement parameters given in refs 24 and 25 were used for fitting of the experimental data and only lattice parameters were refined.

High-pressure angle-dispersive XRD measurements on Li_2MSiO_4 (M = Co, Mn) were carried out with an Xcalibur diffractometer (Oxford Diffraction Ltd.). XRD patterns were obtained on a 135 mm Atlas CCD detector placed at 110 mm from the sample using Mo $K\alpha$ radiation (λ = 0.7107 Å). The X-ray beam was collimated to a diameter of 300 μm. High-pressure measurements on Li_2MSiO_4 powder were performed in a modified Merrill-Bassett diamond anvil cell (DAC) up to 15 GPa. The same setup was previously used to study the high-pressure behavior of ternary oxides in the same pressure range.[26,27] The DACs used have 500 μm of culet size. The Li_2MSiO_4 powder was placed in the 200-μm-diameter holes of the stain-steel gasket preindented to a thickness of 50 μm. A mixture of methanol/ethanol with a ratio of 4:1 was used as the pressure medium, which ensures quasi-hydrostatic conditions up to 10 GPa.[28−30] Ruby chips evenly distributed in the pressure chamber were used to measure the pressure by the ruby fluorescence method.[31] Exposure times were typically of 1 h. The DAC used for these experiments allows access to an angular range 4θ = 50°. The observed intensities were integrated as a function of 2θ in order to give conventional 1D diffraction profiles. The *CrysAlis* software, version 171.34.49, was used for the data collection and preliminary reduction of the data. To analyze the evolution of the lattice parameters with pressure, only the powder patterns below 2θ = 18.3° are considered because of the appearance of the stainless-steel peaks of the gasket. All of the indexations were done using the (010), (011), (111), (210), (020), (002), and (211) reflections to obtain the a, b, and c lattice axes of the $Pmn2_1$ phase of Li_2MnSiO_4 and the (110), (120), (101), (111), (130), (220), (040), (002), and (221) reflections of the $Pbn2_1$ phase of Li_2CoSiO_4.

2.2. Computational Procedures. Investigation of the properties and phase stability of Li_2MSiO_4 is properly achieved within the density functional theory (DFT) method by introducing a Hubbard-like correction term (DFT +U), as has been shown in our previous work.[2,13,14] In this work, the total energies were calculated using the projector augmented wave[32,33] formalism, as implemented in the Vienna Ab Initio Simulation Package[34] with exchange and correlation energies approximated in the generalized gradient approximation (GGA), adding the Hubbard parameter correction (GGA +U) with a J term value of 1 eV and a U value of 5 eV. These values allow the correct reproduction of the lithium intercalation voltages[2,14] and phase stability.[13,14] Other computational details can be found in refs 13 and 14. The initial cell parameters and atomic positions of $Pmn2_1$-Li_2MnSiO_4 and $Pbn2_1$-Li_2CoSiO_4 were taken from refs 24 and 25, respectively. As a first step, the structures were fully relaxed (cell parameters, volume cells, and atomic positions); the final energies of the optimized geometries were recalculated in order to correct for the changes in the basis set of the wave functions during relaxation. In a second step, relaxed structure calculations were performed at various constant volumes and the energy−volume data were fitted to a third-order Birch−Murnaghan equation of state (EOS).

3. RESULTS

3.1. Experimental Part. The room-pressure diffractogram of Li_2MnSiO_4 (Figure 2a) synthesized by hydrothermal
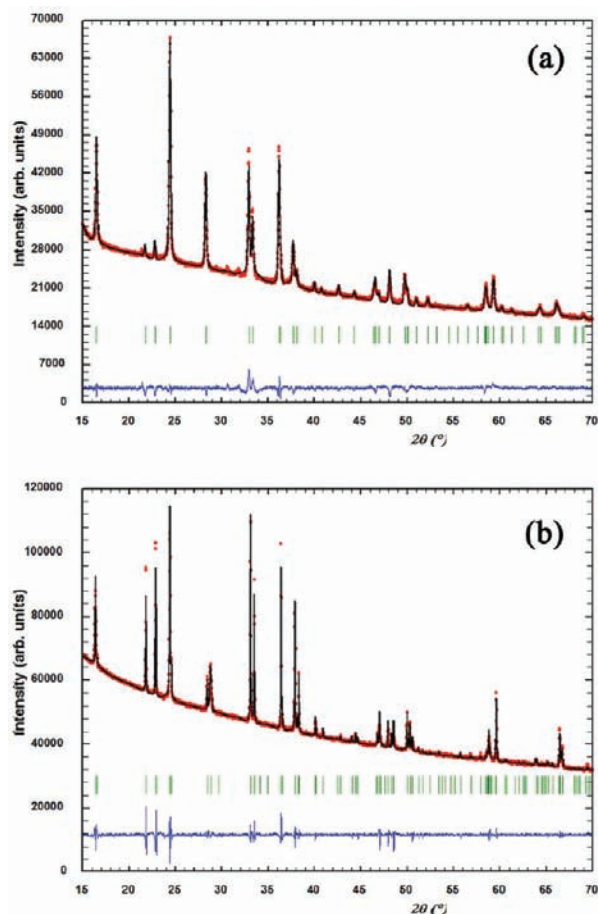
Figure 2. Observed (red) and calculated (black) XRD patterns of as-prepared Li_2MnSiO_4 (a) and Li_2CoSiO_4 (b). Blue is the difference. Vertical bars mark the reflection positions of the (a) $Pmn2_1$ and (b) $Pbn2_1$ phases included in the refinement.

synthesis can be indexed into an orthorhombic structure [space group $Pmn2_1$ (No. 31)], with lattice parameters similar to those previously reported[24] [a = 6.3003(5) Å, b = 5.3678(4) Å, and c = 4.9564(5) Å] and a unit cell volume V = 167.62(5) Å^3. The room-pressure diffractogram of Li_2CoSiO_4 (Figure 2b) can also be indexed into an orthorhombic structure but in a different space group, $Pbn2_1$ (No. 33), with lattice parameters similar to those reported by Yamaguchi et al.:[25] a = 6.2712(3) Å, b = 10.6880(5) Å, c = 4.9333(2) Å, and V = 330.66(4) Å^3.

Figure 3 shows evolution of the XRD patterns of Li_2MnSiO_4 (a) and Li_2CoSiO_4 (b) upon high-pressure conditions. No new Bragg maxima indicative of a phase transition are observed up to 11 GPa. For Li_2CoSiO_4, this result differs from our previous high-temperature, high-pressure quenching experiments, where the $Pmn2_1$ structure was stabilized following treatment at 900 °C and 4 GPa. Not surprisingly, at room temperature, the reconstructive transformation to the $Pmn2_1$ is precluded likely because of the low ionic mobility at room temperature. As seen in Figure 3, above 8 GPa, pressure causes the typical broadening of the Bragg maxima associated with non-hydrostatic stresses in our sample. The shift of the peaks toward higher 2θ angles indicates compression of the structure.
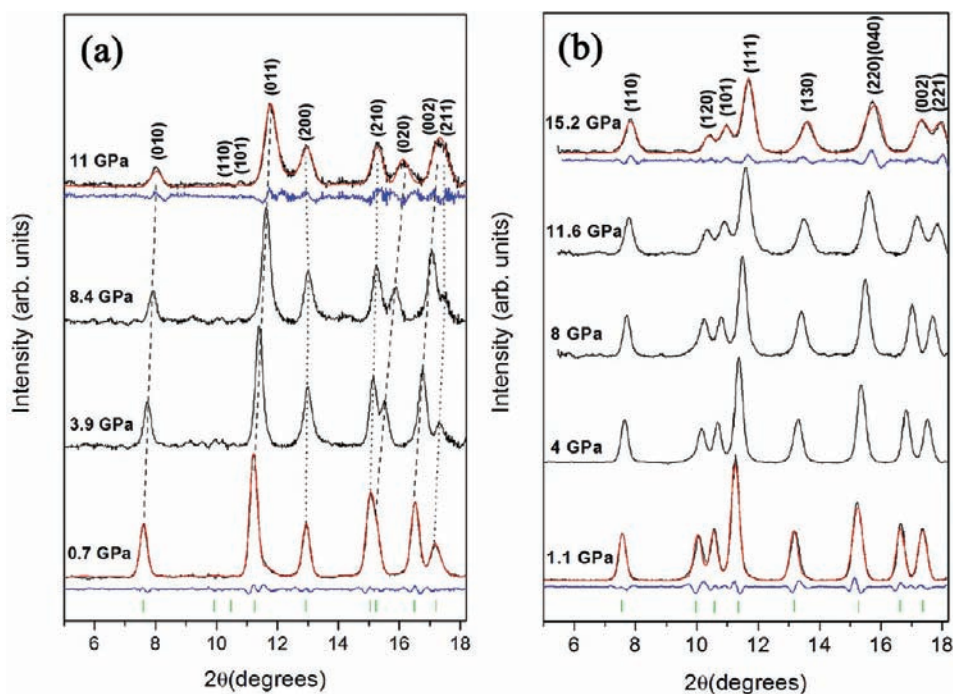
Figure 3. Powder XRD patterns at increasing pressure conditions for (a) Li$_2$MnSiO$_4$ and (b) Li$_2$CoSiO$_4$. Vertical dotted and dashed lines indicate the different 2θ shifts for Bragg reflections that do or do not depend on the a axis, respectively. The LeBail fittings (in red) and differences (in blue) for the low- and high-pressure patterns are also included.
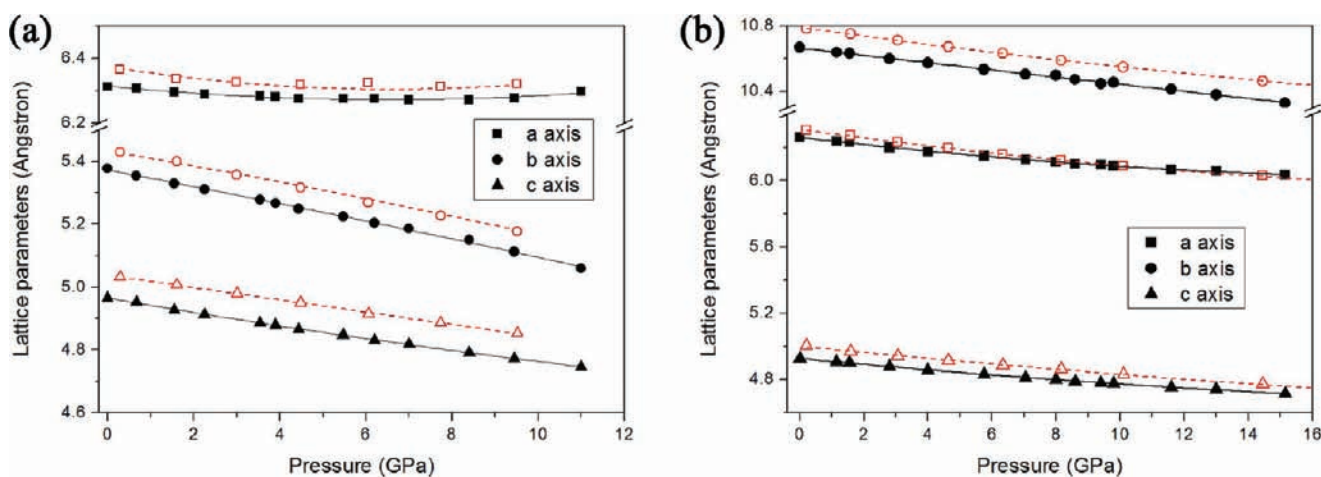
Figure 4. Evolution of the lattice parameters under high pressure for Li$_2$MnSiO$_4$ (a) and Li$_2$CoSiO$_4$ (b). Experimental and theoretical data are represented as black solid and red empty symbols, respectively.

From the XRD data, we obtained the evolution of the volume and lattice parameters of both compounds with pressure. The positions of the different atoms are considered to remain constant with pressure because no significant changes in the relative intensities of the peaks were observed in the XRD patterns. Figure 4 shows variation of the lattice parameters as a function of pressure for manganese and cobalt silicates. For Li$_2$MnSiO$_4$, the a axis has surprising behavior (see Figure 4a). It decreases slightly up to 4.4 GPa, it remains approximately constant with pressure up to 8.5 GPa, and then it shows a negative compressibility, with the a lattice parameter increasing with pressure. This effect can also be easily seen in Figure 3a, where the diffraction peaks corresponding to the crystallographic planes ($h \neq 0$, k, l) show a shift to lower 2θ values with increasing pressure (see the dotted lines). As a

consequence, a splitting of the (210) and (020) Bragg peaks can be observed for Li$_2$MnSiO$_4$. The absolute contractions for a, b, and c between room pressure and 11 GPa are 0.015, 0.318, and 0.22 Å, respectively. When analyzed in relative terms, these variations are 0.24, 5.91, and 4.43%, respectively, indicating that compression is highly anisotropic. On the contrary, variation of the lattice constants of the β phase of Li$_2$CoSiO$_4$ with pressure is only slightly anisotropic (Figure 4b). For instance, the absolute contractions for a, b, and c between room pressure and 9.2 GPa are 0.1654, 0.2215, and 0.1464 Å, respectively. However, when analyzed in relative terms, these variations are 2.64, 2.08, and 2.97%, respectively, indicating that compression is rather isotropic.

Figure 5 shows the fitting of the variation of the volumes with pressure to a third-order Birch−Murnaghan EOS, where
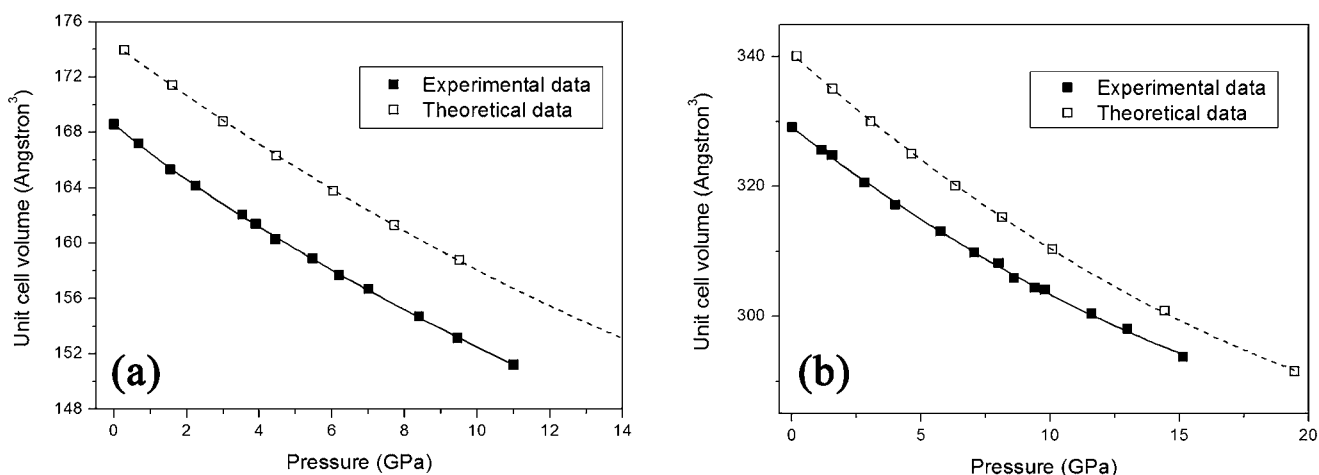
Figure 5. Fitting of the volume variation with pressure to a third-order Birch–Murnaghan EOS for (a) Li_2MnSiO_4 and (b) Li_2CoSiO_4.

the values of the bulk modulus (B_0) and its derivative with pressure (B_0') are left to vary freely. The obtained characteristic parameters are $B_0 = 81(1)$ GPa and $B_0' = 4.1(3)$ and $B_0 = 95(3)$ GPa and $B_0' = 5.2(8)$ for Li_2MnSiO_4 and Li_2CoSiO_4, respectively. Interestingly, these values are lower than those found in other orthosilicates (olivine-Fe_2SiO_4, $B = 113$ GPa; phenakite-Be_2SiO_4, $B = 201.8$ GPa; garnet-$Ca_3Fe_2Si_3O_{12}$, $B = 159$ GPa, and so forth), which suffer a pressure-driven polymorphic transformation.[35,36] These small values of the bulk moduli seem to be intimately related with the amount of lithium atoms in the structure, as discussed below. Du and René Corrales reported moderate B values of ~70 GPa for the minerals Li_2SiO_3 and $Li_2Si_2O_5$.[37]

3.2. Computational Part. First-principles calculations allow investigation of the behavior under pressure of existing and virtual Li_2MSiO_4 polymorphs. Aiming to investigate the effect of the composition and crystal structure on the high-pressure behavior of the Li_2MSiO_4 family, we have completed the experimental results of $Pmn2_1$-$LiMnSiO_4$ and $Pbn2_1$-Li_2CoSiO_4 with those of potential $Pbn2_1$-Li_2MnSiO_4 and $Pmn2_1$-Li_2CoSiO_4 compounds.

Figure 6 (left axis) shows the calculated total energy as a function of the volume for Li_2MnSiO_4 and Li_2CoSiO_4 polymorphs together with the EOS fitting. The parameters of the fitting are listed in Table 1. The calculated bulk moduli are in qualitative agreement with the experimental results. The manganese polymorphs are slightly softer than the cobalt polymorphs. In both silicates, the $Pmn2_1$ phase, which is the densest form, has a larger bulk modulus. Figure 6 also shows that the predicted relative stability of $Pmn2_1$ and $Pbn2_1$ is opposite for cobalt and manganese. Indeed, a recent DFT investigation[14] shows that the relative energetic stability of polymorphs in the Li_2MSiO_4 family is largely controlled by the size of the M ion, with the smallest cations preferring the $Pbn2_1$ structure to diminish electrostatic repulsions. In Figure 6a, it can be seen that, for Li_2MnSiO_4, the $Pbn2_1$ polymorph is less stable than the $Pmn2_1$ form (0.043 eV/fu), in accordance with experiments; while $Pmn2_1$ is a frequent polymorph for Li_2MnSiO_4 for samples obtained at low temperatures, the $Pbn2_1$ form has never been found experimentally.[1,13,24] $Pbn2_1$ is the most stable polymorph of Li_2CoSiO_4 at ambient pressure (0.029 eV/fu; see Figure 6b), in good agreement with the experiments.[10] At sufficiently high pressure, on the order of 4 GPa, calculations indicate that the $Pmn2_1$ form becomes the
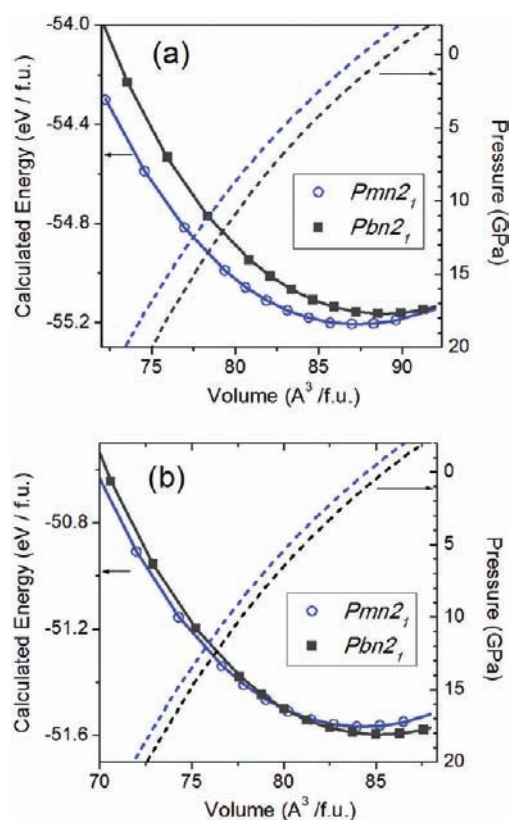
Figure 6. Left axis: Calculated total energies versus volume and fitting of the energy–volume data to the Birch–Murnaghan EOS. Right axis: Volume dependence with pressure according with the EOS fitting for (a) Li_2MnSiO_4 and (b) Li_2CoSiO_4.

thermodynamically stable form. Indeed, we have previously shown that $Pmn2_1$-Li_2CoSiO_4 can be stabilized following the high-pressure, high-temperature treatment of other Li_2CoSiO_4 polymorphs.[38] However, in the present in situ room-temperature investigation, that transformation is not observed. Transformations upon pressure to the thermodynamically stable forms ($Pbn2_1 \rightarrow Pmn2_1$ in the present case) are typically difficult at low temperature because of kinetic barriers.

Calculated variation of the lattice parameters with pressure for the known polymorphs $Pmn2_1$-Li_2MnSiO_4 and $Pbn2_1$-Li_2CoSiO_4 have been compared to the experimental data in

Table 1. Calculated EOS Parameters for Li$_2$MSiO$_4$ (M = Mn, Co) Polymorphs (Experimental Values Are Given in Parentheses)

M in Li$_2$MSiO$_4$	structural type	bulk modulus (GPa)	bulk derivative with pressure	equilibrium volume (A^3/fu)	equilibrium energy (eV/fu)
Mn	$Pmn2_1$	83.9 (81)	3.7 (4.1)	87.29	−55.207
	$Pbn2_1$	80.6	4.3	88.92	−55.164
Co	$Pmn2_1$	90.6	4.0	84.29	−51.567
	$Pbn2_1$	88 (95)	4.2 (5.2)	85.20	−51.596
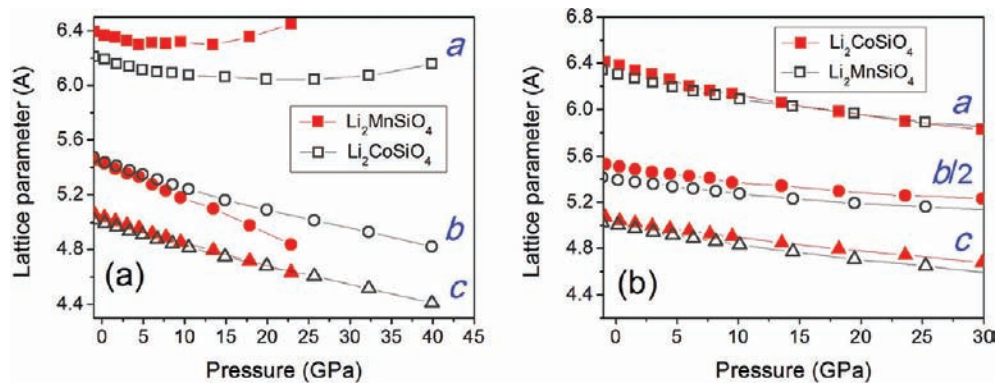
Figure 7. Calculated lattice parameter variation as a function of the pressure for Li$_2$MnSiO$_4$ and Li$_2$CoSiO$_4$ crystallizing in space groups $Pmn2_1$ (a) and $Pbn2_1$ (b). The a, b, and c lattice parameters are represented by squares, circles, and triangles, respectively.

Figure 4. There is a good qualitative agreement. The computational data correctly reproduce the highly anisotropic compression of the lattice parameters for Li$_2$MnSiO$_4$, with variations of 0.9 (a), 5.1 (b), and 4.0% (c). Expansion of the a axis is also well captured by the DFT. Therefore, theoretical calculations rule out that the nonlinear compression of the a axis could be caused by nonhydrostatic stresses. For $Pbn2_1$-Li$_2$CoSiO$_4$, variation of the lattice parameters between 0 and 9.2 GPa [3.3% (a), 2.2% (b), and 3.4% (c)] also follows the experimentally observed trends.

Calculated variation of the lattice parameters with pressure for Li$_2$MSiO$_4$ (M = Co, Mn) within $Pmn2_1$ and $Pbn2_1$ is depicted in Figure 7. For a given polymorph, the predicted behavior under pressure is independent of the nature of the M cation. The densest $Pmn2_1$ polymorphs show a highly anisotropic behavior with an unusual expansion of the a lattice at high pressures. Expansion of the a lattice parameter is predicted to initiate at about 5 and 18 GPa for manganese and cobalt, respectively. The lower pressure for managanese silicate might be related to its softer character (lower bulk modulus). As shown in Figure 1, in the $Pmn2_1$ polymorph, the [SiO$_4$] and [MO$_4$] tetrahedra alternate along the a axis. It has been recently shown that electrostatic repulsion between the M and silicon cations plays an important role in the energetics of Li$_2$MSiO$_4$ polymorphs.[14] The volume contraction induced by pressure would increase the cationic repulsion existing between the neighboring silicon and transition metal (TM) ions in the $Pmn2_1$ polymorph. It is quite likely that enlargement of the a lattice parameter helps to diminish these repulsions. The lattice parameter variation for the more open $Pbn2_1$ polymorph is independent of the TM ions. In this structure, the TM ions and silicon do not alternate along the crystallographic axis, and the structure can hold the volume contraction without excessive cation repulsion.

Regardless the unusual expansion of the a lattice parameter, the $Pmn2_1$ host remains stable up to a pressure of 11 GPa. Previous high-temperature, high-pressure quenching experiments also failed to induce phase transformation of the $Pmn2_1$

polymorph. This contrasts with well-known phase transformations of other silicates with larger bulk moduli. The moderate bulk modulus of Li$_2$MSiO$_4$ is associated with the presence of lithium in the structure, as inferred from calculated variation of the bond lengths under pressure (Figure 8). The
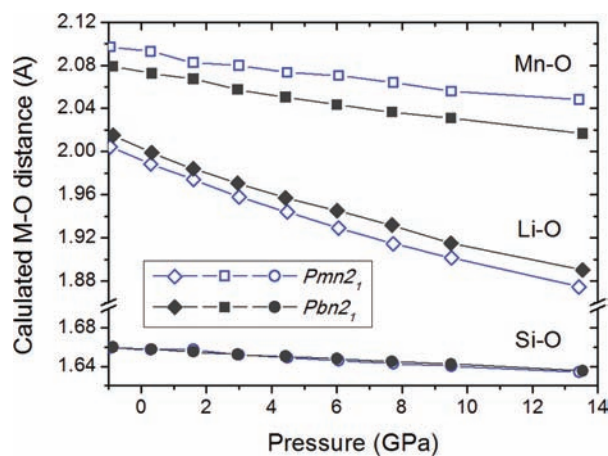
Figure 8. Calculated M−O bond lengths as a function of the pressure for Li$_2$MnSiO$_4$ crystallizing in space groups $Pmn2_1$ (solid symbols) and $Pbn2_1$ (empty symbols).

Li−O bonds are twice as compressible as the Mn−O bonds for both $Pmn2_1$ and $Pbn2_1$ polymorphs. Because the Si−O units are quite rigid, the Li−O bonds are by far the most compressible bonds. Thus, the fact that the [MSiO$_4$] layers are parallel to the ac plane and connected by [LiO$_4$] tetrahedra entails that the b axis should be the most compressible axis, as indeed happens. What's more, the bulk compressibility seems to be mainly determined by compression of the [LiO$_4$] tetrahedra. This would explain the similar bulk moduli of Li$_2$MnSiO$_4$ and Li$_2$CoSiO$_4$, also similar to that of Li$_2$SiO$_3$. In contrast, other silicates that do not contain lithium usually have larger bulk moduli because all of their polyhedral units are much less compressible than [LiO$_4$]. Additionally, the bulk compressi-

bility of the Li_2MSiO_4 silicates could be directly correlated to the compressibility of the $[LiO_4]$ tetrahedra using the model developed by Hazen et al.[39] and recently updated by Errandonea and Manjón,[40] where the B_0 value of the compound is calculated from the cation charge density per unit volume of the most compressible polyhedra: B_0 (GPa) = $610Z_i/d^3$ ($Z_i = 1$ is the lithium formal charge, and d is the mean value of the Li−O bond distance in angstroms). In such a case, the estimated bulk moduli are 78 and 81 GPa for Li_2MnSiO_4 and Li_2CoSiO_4, respectively, which would confirm that the pressure behavior of the studied structures is basically controlled by the $[LiO_4]$ tetrahedra.

In spite of the good compressibility of the framework, it is likely that a densification of the structure would be energetically unfavorable. Indeed, if the composition Li_2MSiO_4 (AB type) adopted a cubic close packing structure, the Li^+, M^{2+}, and Si^{4+}, cations would occupy edge-sharing octahedral voids producing a large electrostatic repulsion.

4. CONCLUSIONS

The structural degradation of Li_2MSiO_4 cathode materials upon removal of high lithium contents is inherent to the distorted hexagonal oxygen packing of the known polymorphs, where M ions are constrained to occupy tetrahedral sites. Structural modifications could lead to Li_2MSiO_4 materials with better electrochemical properties. In the present work, we have investigated the possibility of high pressure as a route to promoting a cubic oxygen packing.

Although the Li_2MSiO_4 silicates exhibit moderate bulk moduli (on the order of 90 GPa), no phase transformation is detected up to 15 GPa at room temperature. An unusual enlargement of the a axis is observed for the denser $Pmn2_1$-Li_2MnSiO_4 polymorph. Such behavior is also predicted for the isostructural Li_2CoSiO_4 phase at higher pressures. We conclude that the difficulty in preparing novel high-pressure polymorphs of Li_2MSiO_4 is not attributable to the low compressibility of the Li_2MSiO_4 structures but rather to the strong cationic repulsion that would exists in the denser forms. It is therefore quite complicated to stabilize the composition Li_2MSiO_4 (with a large cation/anion ratio) in packings other than a tetrahedral one. This leads to chemical modifications as the most promising route to improving the electrochemical performance of the Li_2MSiO_4 family of compounds.

■ AUTHOR INFORMATION

Corresponding Author
*E-mail: dsantamaria@quim.ucm.es.

Notes

The authors declare no competing financial interest.
‡MALTA Consolider Team.

■ ACKNOWLEDGMENTS

■ REFERENCES

(1) Islam, M. S.; Dominko, R.; Masquelier, C.; Sirisopanaporn, C.; Armstrong, A. R.; Bruce, P. *J. Mater. Chem.* **2011**, DOI: 10.1039/c1jm10312a.

(2) Arroyo y de Dompablo, M. E.; Armand, M.; Tarascon, J.-M.; Amador, U. *Electrochem. Commun.* **2006**, 8, 1292−1298.

(3) Armand, M.; Arroyo y de Dompablo, M. E. *J. Mater. Chem.* **2011**, 21, 10026−10034.

(4) Kokalj, A.; Dominko, R.; Mali, G.; Meden, A.; Gaberscek, M.; Jamnik, J. *Chem. Mater.* **2007**, 198, 3633−3640.

(5) Nyten, A.; Kamali, S.; Haggstronm, L.; Gustafsson, T.; Thomas, J. O. *J. Mater. Chem.* **2006**, 16, 2266−2272.

(6) West, A. R.; Bruce, P. *Acta Crystallogr., Sect. B* **1982**, 38, 1891−1896.

(7) Santamaria-Perez, D.; Vegas, A.; F. Liebau, F. *Struct. Bonding (Berlin)* **2005**, 118, 121−177.

(8) Liebau, F. *Structural Chemistry of Silicates: Structure, Bonding and Classification*; Springer: Berlin, 1985.

(9) Baur, W. H.; McLarnan, T. J. *J. Solid State Chem.* **1982**, 42, 300−321.

(10) Armstrong, A. R.; Lyness, C.; Menetrier, M.; Bruce, P. *Chem. Mater.* **2010**, 22, 1892−1900.

(11) West, A. R.; Glasser, F. P. *J. Solid State Chem.* **1972**, 4, 20−28.

(12) Mali, G.; Sirisopanaporn, C.; Masquelier, C.; Hanzel, D.; Dominko, R. *Chem. Mater.* **2011**, 23, 2735−2744.

(13) Arroyo y de Dompablo, M. E.; Dominko, R.; Gallardo-Amores, J. M.; Dupont, L.; Mali, G.; Ehrenberg, H.; Jamnik, J.; Moran, E. *Chem. Mater.* **2008**, 20, 5574−5584.

(14) Saracibar, A.; Van de Ven, A.; Arroyo y de Dompablo, M. E. *Chem. Mater.* **2012**, in press.

(15) Santamaria-Perez, D.; Liebau, F. *Struct. Bonding (Berlin)* **2011**, 13, 1−29.

(16) Santamaria-Perez, D.; Vegas, A. *Acta Crystallogr., Sect. B* **2003**, 59, 305−323.

(17) Klaska, R.; Jarchow, O. *Z. Kristallogr.* **1975**, 142, 225−238.

(18) Kerr, I. S. *Z. Kristallogr.* **1974**, 139, 186−195.

(19) Dickinson, R. G.; Friauf, J. B. *J. Am. Chem. Soc.* **1924**, 46, 2457−2462.

(20) Sirisopanaporn, C.; Boulineau, A.; Hanzel, D.; Dominko, R.; Budic, B.; Armstrong, A. R.; Masquelier, C. *Inorg. Chem.* **2010**, 49, 7446−7451.

(21) Arroyo y de Dompablo, M. E.; Gallardo-Amores, J. M.; Garcia-Martinez, J.; Moran, E.; Tarascon, J.-M.; Armand, M. *Solid State Ionics* **2008**, 179, 27−32.

(22) Mali, G.; Meden, A.; Dominko, R. *Chem. Commun.* **2010**, 46, 3306−3308.

(23) Rodriguez-Carvajal, J. *Phys. Rev. B* **1993**, 192, 55−69.

(24) Dominko, R.; Bele, M.; Gaberscek, M.; Meden, A.; Remskar, M.; Jamnik, J. *Electrochem. Commun.* **2006**, 8, 217−222.

(25) Yamaguchi, A.; Akatsuka, K.; Setoguchi, M.; Takaki, Y. *Acta Crystallogr., Sect. B* **1979**, 35, 2680−2682.

(26) Errandonea, D.; Santamaria-Perez, D.; Bondarenko, T.; Khyzhun, O. *Mater. Res. Bull.* **2010**, 45, 1732−1735.

(27) Santamaria-Perez, D.; Gracia, L.; Garbarino, G.; Beltrán, A.; Chuliá-Jordán, R.; Gomis, O.; Errandonea, D.; Ferrer-Roca, C.; Martínez-García, D.; Segura, A. *Phys. Rev. B* **2011**, 84, 054102.

(28) Errandonea, D.; Meng, Y.; Somayazulu, M.; Häusermann, D. *Physica B* **2005**, 355, 116−125.

(29) Klotz, S.; Chervin, J. C.; Munsch, P.; Le Marchand, G. *J. Phys. D* **2009**, 42, 075413.

(30) Iizuka, R.; Kagi, H.; Komatsu, K. *J. Phys.: Conf. Ser.* **2010**, 215, 012177.

(31) Mao, H. K.; Xu, J.; Bell, P. M. *J. Geophys. Res., Solid Earth Planet.* **1986**, 91, 4673−4676.

(32) Blochl, P. E. *Phys. Rev. B* **1994**, 50, 17953−17979.

(33) Kresse, G.; Joubert, J. *Phys. Rev. B* **1999**, 59, 1758−1775.

(34) Kresse, G.; Furthmuller, J. *Comput. Mater. Sci.* **1996**, 6, 15−50.

(35) Smyth, J. R.; Jacobsen, S. D.; Hazen, R. M. *High-temperature and high-pressure crystal chemistry*; The Mineralogical Society of America: Washington, DC, 2000; Vol. *41*.

(36) Navrotsky, A. *Prog. Solid State Chem.* **1987**, *17*, 53−86.

(37) Du, J.; René Corrales, L. *J. Phys. Chem.* **2006**, *110*, 22346−22352.

(38) Arroyo y de Dompablo, M. E.; Amador, U.; Gallardo-Amores, J. M.; Moran, E.; Ehrenberg, H.; Dupont, L.; Dominko, R. *J. Power Sources* **2009**, *189*, 638−642.

(39) Hazen, R. M.; Finger, L. W.; Mariathasan, J. W. E. *J. Phys. Chem. Solids* **1985**, *46*, 253−263.

(40) Errandonea, D.; Manjón, F. J. *Prog. Mater. Sci.* **2008**, *53*, 711−773.

5786

dx.doi.org/10.1021/ic300320r | *Inorg. Chem.* 2012, 51, 5779−5786